

Dielectric Spectroscopy of Ferroelectric Crossbred PVDF–TiO₂ Polymer Composite Thin Films

A. H. Arshad¹, S. Dani¹, S. S. Kulkarni², U. V. Khadke^{1*}

¹Department of Physics, Vijayanagara Sri Krishnadevaraya University, Bellary-583105, Karnataka, India

²Department of Physics, KLS Gogte Institute of Technology, Belagavi-590006, India

Received 8 June 2022, accepted in final revised form 24 October 2022

Abstract

Polyvinylidene fluoride (PVDF) ferroelectric polymer blend with titanium dioxide (TiO₂) is synthesized in the form of thin films by solution casting method. The synthesized PVDF-TiO₂ composite films with a different wt% of TiO₂ (2, 4, 6, 8, and 10) as fillers in the PVDF matrix were characterized by X-ray diffraction (XRD), scanning electron microscope (SEM) and Fourier Transform Infrared (FTIR) spectroscopy. The XRD patterns of PVDF-TiO₂ composite films confirmed the existence of a β -phase PVDF, uniform distribution of TiO₂ particles in the polymer matrix and the crystallinity of the polymer composites was found to be enhanced. The SEM micrograph depicts the augmentation in the structural density due to the addition of TiO₂ particles in the PVDF matrix. The dielectric constant of the PVDF-TiO₂ films is found to be an anomaly at lower frequencies and decreases with an increase in frequency agreeing with the Maxwell–Wagner type of interfacial polarization. The enhancement in the dielectric constant of PVDF-TiO₂ composites at lower frequencies suggests that the prepared polymer composite thin films are useful as separator membranes in energy storage devices.

Keywords: Ferroelectric polymer; PVDF-TiO₂; Dielectric constant.

© 2023 JSR Publications. ISSN: 2070-0237 (Print); 2070-0245 (Online). All rights reserved.
doi: <http://dx.doi.org/10.3329/jsr.v15i1.60132> J. Sci. Res. **15** (1), 95-102 (2023)

1. Introduction

Polymers have been identified as a significant functional material because of their promising barrier qualities, ease of modification, and wide range of technological usage [1]. Polymer composites provide a large scale of properties, such as stability, good strength, tolerable resistance to weariness and corrosion, ease to fabricate in the desired shape, lightweight, high flexibility in designing, and can be achieved desired thermal properties. Further, these properties can be tuned according to our requirements by incorporating appropriate dopants as fillers in the polymer matrix. Polymer composites

* Corresponding author: khadke@vskub.ac.in

are in-demand in different fields such as automobile, aerospace, medical, electronic applications, marine, military, and energy [2]. Ferroelectric fluorinated fluoropolymers have rapidly developed their prospects of application in numerous aspects. Among the various ferroelectric fluoropolymers, polyvinylidene fluoride (PVDF) with β -phase exhibits semi-crystallinity with a repeated unit of $\text{CH}_2\text{-CF}_2$ [3]. The ferroelectric PVDF is well known for its lower acoustic impedance, lesser dissipation factor, and high permittivity [4]. Due to its higher magnetic activity, PVDF as a binder improves the ability of electromagnetic waves to be sensed. [5]. Organic-inorganic nanocomposites have recently generated a lot of interest in the research of their dielectric properties due to their sustained spontaneous polarisation which causes high dielectric and lowers energy loss that extended its applications in energy storage devices, memory devices, sensors, actuators, etc. [6-8].

There are various techniques to increase the hydrophilic nature of PVDF membranes. TiO_2 is one such hydrophilic material, possessing intriguing chemical, electrical, and optical properties. TiO_2 is added to the PVDF matrix to increase its effectiveness by reducing the fouling effect. TiO_2 has attracted the most attention than other materials as it has a higher band gap of around 3.2 eV, a high refractive index of 2.3, possesses transparency in the visible range, exhibits a high dielectric constant, and can be easily doped with active ions [9,10].

PVDF- TiO_2 composite materials are being considered for various optical applications such as in multilayer optical filters, gas sensors, antireflective coating, photocatalysts, planar waveguide stability [11-13], antibacterial and UV-cleaning properties [14,15-17]. These composites are also affordable and simple to create in any desired shape using different techniques such as solvent casting, compression molding, hot pressing, and ball milling. By varying the filler concentration, the qualities of the composite materials can be customized based on requirements to improve performance. A high level of dispersion of the fillers in the matrix has been found to increase the performance of composites in photoelectron-chemical devices, electrochemical devices, nonlinear optical systems, and other applications [18-22].

In this paper, we report the method of synthesis of thin films of ferroelectric polymer PVDF- TiO_2 composites by solution casting method using N-N-dimethylacetamide (DMAC) as a solvent. Structural and surface morphology of prepared PVDF and PVDF- TiO_2 composite thin films were carried out using an XRD unit and scanning electron microscopy (SEM) respectively. Functional groups and material molecular composition of PVDF-based composite films were obtained using FTIR spectra. Maxwell-Wagner type of interfacial polarization is validated by the electrical properties, such as dielectric behavior via capacitance, which has been measured using an LCR (Inductance Capacitance and Resistance) meter.

2. Materials and Method

2.1. Materials

PVDF in the form of granular having a molecular weight 534000 GPC was purchased from Sigma Aldrich, India. AR grade TiO_2 and DMAC procured from SD-Fine Chem. Ltd. Mumbai, India was used in the preparation of PVDF and PVDF- TiO_2 composite thin films. XRD (Rigaku Miniflex 5th Gen, Japan), FTIR (Perkin Elmer Spectrum Two L160000U, USA), SEM (ZEISS Sigma, Germany) and LCR meter (Hioki IM3536, Japan) were used for characterizations.

2.1. Preparation of PVDF and PVDF- TiO_2 composite films

Pure PVDF and PVDF- TiO_2 composite films were made using a simple and inexpensive solution casting technique, as shown in Fig. 1 [23]. PVDF was appropriately dissolved in 50 mL of DMAC solvent, and the mixture was then heated at 40 °C on a magnetic stirrer hot plate to form a transparent homogeneous solution. The mixture was put into a petridish and allowed to dry for 24 h while exposed to light. The film obtained was peeled off. By incorporating TiO_2 powder into the PVDF solution in wt% of 2, 4, 6, 8, and 10, the standardized PVDF- TiO_2 solution is created. To ensure that the particles in the homogeneous solution were evenly distributed throughout the polymer matrix, it was sonicated for 30 min before being put into the petridish.

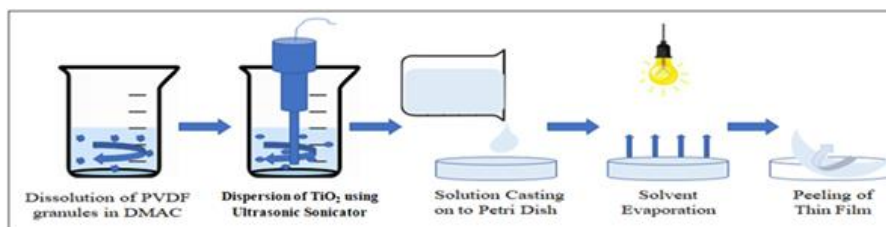


Fig. 1. Solution casting method for obtaining thin films.

3. Results and Discussion

3.1. XRD analysis

The XRD pattern of pristine PVDF film is shown in Fig. 2. The peak positions at 2θ values of 18.48° and 20.18° corresponds to (020) and (110) planes respectively, and their relative intensities represent the presence of β -phase with a minute trace of α -phase. This is in good agreement with the reported literature [24].

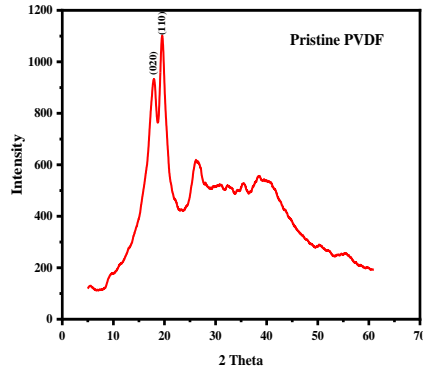


Fig. 2. XRD pattern of pristine PVDF film.

Fig. 3 shows the XRD pattern of PVDF- TiO₂ composites of different weight percentages. The diffraction angles 25.25°, 26.6°, 37.85°, 39.3°, 48.1°, 53.95°, and 55.05° corresponds to the (101), (110), (103), (004), (200), (105), and (201) respectively, representing the lattice planes of anatase phase TiO₂ (JCPDS-211272). It is observed from the XRD patterns that as the wt% of TiO₂ increased, the semi-crystallinity of the PVDF decreased and the crystallinity of TiO₂ increased, and was found maximum for 10 wt% [25].

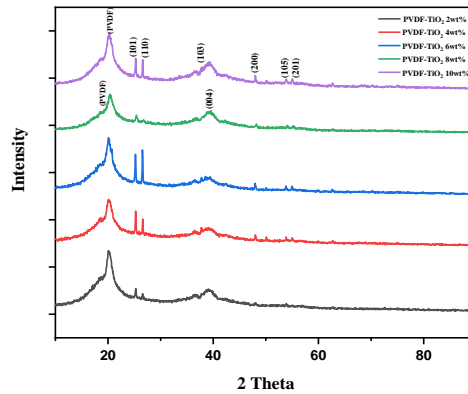


Fig. 3. XRD pattern of PVDF-TiO₂ composite films.

Fig. 4(a-e) depicts the SEM images of PVDF-TiO₂ composites containing different wt% (2, 4, 6, 8, and 10) of TiO₂. It is observed that with the increase in the wt% of TiO₂ in the PVDF matrix, the pore size of the membrane has decreased. TiO₂ particles tend to occupy the pores leading to the increase in the structural density [26].

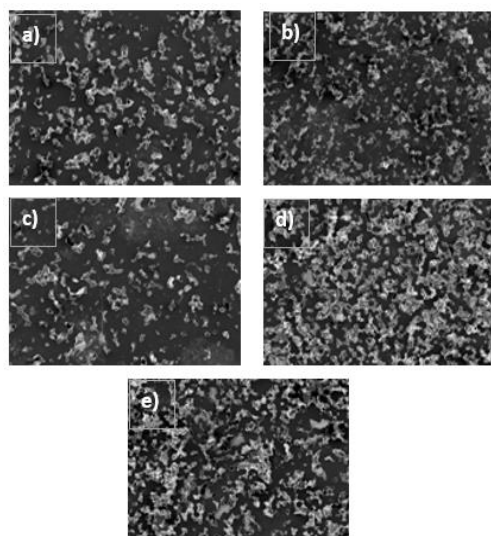


Fig. 4. SEM Micrographs of PVDF-TiO₂ composite films at different wt% of TiO₂: a) 2, b) 4, c) 6, d) 8 and e) 10.

Fig. 5 shows the FTIR spectra of PVDF-TiO₂ composites. An examination of the FTIR spectra of PVDF-TiO₂ composites reveals that the region 1450 to 1000 cm⁻¹ represents the continuous band absorption region which corresponds to fluorocarbon absorption (C-F). The entire characteristic vibrational bands (480, 510, 840, 882 cm⁻¹) represent that the PVDF matrix is in β-phase. The peaks at 625 cm⁻¹, 783 cm⁻¹, and 927 cm⁻¹ are due to the trace of the α-phase present in the PVDF matrix. This report is in agreement with XRD results. The prominent signal at 1383 cm⁻¹ is related to Ti-O modes [27,28]. Peaks at 417 cm⁻¹, 455 cm⁻¹, and 1416 cm⁻¹ are evidence of the stretching vibrational modes of the Ti-O, and Ti-O-Ti bonds respectively [29].

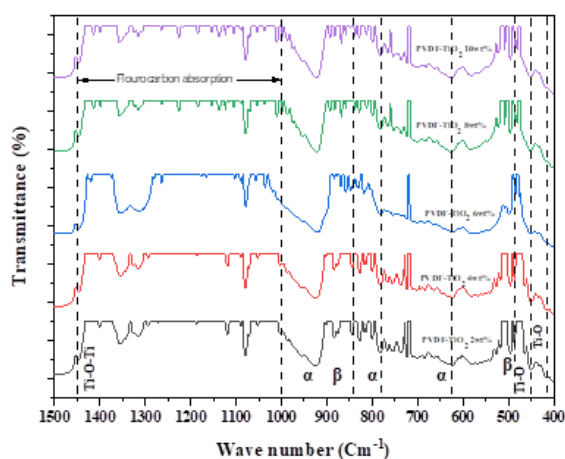


Fig. 5. FTIR spectra of PVDF-TiO₂ composites.

Fig. 6 depicts the variation of the dielectric constant of PVDF-TiO₂ composites thin film with frequency. In the frequency range of 50 Hz to 1 MHz, the dielectric constant decreased with the increase in frequency for all samples of PVDF-TiO₂ composites but there is a rapid fall in the dielectric constant in the range of 50 Hz to 500 Hz for all samples. In the frequency range of 500 Hz to 10 kHz, the variation of dielectric constant is observed as shown in inset Fig. 6. The increase in dielectric constant for the PVDF-TiO₂ composites (2, 6 and 8 wt%) at a frequency higher than 20 kHz need to be understood in terms of dipole switching dielectric constant of PVDF-TiO₂ composites with wt% of TiO₂ at three different frequencies of 50Hz, 100Hz, and 1kHz. The dielectric constant increased linearly with increase in wt% of TiO₂ filler for 2, 4 and 6 wt% at the frequencies of 50Hz and 100Hz. Beyond 6 wt% of TiO₂, the dielectric constant decreased at 100 Hz frequency. However, the dielectric constant for the higher concentrations of TiO₂ (8 and 10 wt%) is almost saturated at frequencies beyond 1 kHz [30]. The abrupt increase in the dielectric constant for PVDF-TiO₂ composites in the low-frequency region is due to the contributions of space charges layers trapped at the interface between the inclusions and the polymer matrix in the composite resulting in an increase of the bound charges on the electrodes in phase with the applied electric field E, which is known as the Maxwell-Wagner effect [31].

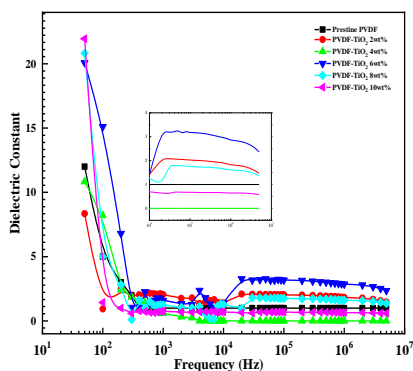


Fig. 6. Variation of dielectric constant with respect to frequency.

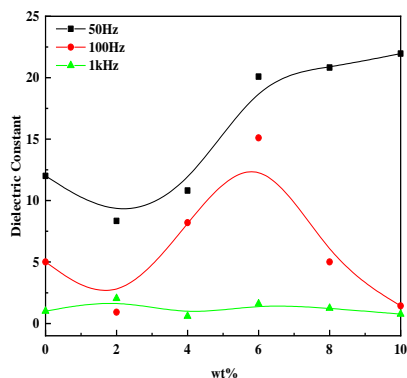


Fig. 7. Variation of dielectric constant with respect to wt% TiO₂ in PVDF-TiO₂ composites.

4. Conclusion

The PVDF and PVDF-TiO₂ polymer composite thin films of different stoichiometric ratios were prepared by the simple solvent casting method. The β -phase dominant PVDF composite films are evidenced by the XRD pattern. FTIR spectra described the characteristic vibrational bands (480, 510, 840, 882 cm⁻¹) representing the PVDF matrix in β -phase and the stretching vibrational modes of the Ti-O, Ti-O, and Ti-O-Ti bonds confirmed the chemical composition of the thin films. The structural density of the films increased as the concentration of TiO₂ increased in PVDF. The incorporation of 2-6 wt%

TiO₂ particles in the PVDF matrix enhanced the dielectric constant at lower frequencies and gets saturated for the higher concentration of TiO₂ in PVDF. This suggests that the small addition of TiO₂ particles in PVDF increases the structural density of the film. The high dielectric constant at a concentration between 2-6 wt% is due to interfacial polarization which validates the Maxwell –Wagner effect. Therefore, the prepared PVDF-TiO₂ composite thin films having high dielectric constant and structural densities can be used for storage devices.

Acknowledgments

The authors acknowledge Y. T. Ravikiran, Department of Physics, Govt. Science College and PG Center, Chitradurga, Karnataka for laboratory support to study dielectric property. The authors also thank IUAC, New Delhi for research grants under project UFR 70320.

References

1. S. Mathai and P. S. Shaji, J. Sci. Res. **14**, 973 (2022). <https://doi.org/10.3329/jsr.v14i3.58338>
2. I. O. Oladele, T. F. Omotosho, and A. A. Adediran, Int. J. Polym. Sci. **2020**, ID 8834518 (2020). <https://doi.org/10.1155/2020/8834518>
3. T. Furukawa, M. Date, and E. Fukada, J. Appl. Phys. **51**, 1135 (1980). <https://doi.org/10.1063/1.327723>
4. R. Gregorio and M. Cestari, J. Polym. Sci. Part B: Polym. Phys. **32**, 859 (1994). <https://doi.org/10.1002/polb.1994.090320509>
5. Q. M. Zhang, H. F. Li, M. Poh, X. Feng, Z. Y. Cheng, H. S. Xu, and C. Huang, Nature **419**, 284 (2002). <https://doi.org/10.1038/nature01021>
6. W. Xia, and Z. Zhang, IET Nanodielectrics **1**, 17 (2018). <https://doi.org/10.1049/iet-nde.2018.0001>
7. J. Yanda, M. Zhou, Z. Shen, X. Zhang, H. Pan, and Y. -H. Lin. APL Mater. **9**, ID 020905 (2021). <https://doi.org/10.1063/5.0039126>
8. S. Liu, J. T. Kim, and S. J. Kim, Food Sci. **73**, 143 (2008). <https://doi.org/10.1111/j.1750-3841.2008.00699.x>
9. H. P. Ngang, B. S. Ooi, A. L. Ahmad, and S. O. Lai, Chem. Eng. J. **197**, 359 (2012). <https://doi.org/10.1016/j.cej.2012.05.050>
10. D. P. Partlow and T. W. ÓKeeffe, Appl. Optics **29**, 1526 (1990). <https://doi.org/10.1364/AO.29.001526>
11. S. -S. Lin and D. -K. Wu, Cer. Int. **36**, 87 (2010). <https://doi.org/10.1016/j.ceramint.2009.06.023>
12. L. Yang, S. S. Saavedra, N. R. Armstrong, and J. Hayes, Anal. Chem. **66**, 1254 (1994). <https://doi.org/10.1021/ac00080a010>
13. J. -H. Li, Y. -Y. Xu, L. -P. Zhu, J. -H. Wang, C. -H. Du, J. Membr. Sci. **326**, 659 (2009). <https://doi.org/10.1016/j.memsci.2008.10.049>
14. A. Rahimpour, M. Jahanshahi, B. Rajaeian, and M. Rahimnejad, Desalination **278**, 343 (2011). <https://doi.org/10.1016/j.desal.2011.05.049>
15. S. S. Madaeni and N. Ghaemi, J. Membr. Sci. **303**, 221 (2007). <https://doi.org/10.1016/j.memsci.2007.07.017>
16. R. A. Damodar, S. -J. You, and H. -H. Chou, J. Hazard. Mater. **172**, 1321 (2009). <https://doi.org/10.1016/j.jhazmat.2009.07.139>

17. S. V. Anand and D. R. Mahapatra, *Nanotechnology* **20**, ID 145707 (2009).
<https://doi.org/10.1088/0957-4484/20/14/145707>
18. S. V. Anand and D. R. Mahapatra, *Smart Mater. Struct.* **18**, ID 045013 (2009).
<https://doi.org/10.1088/0964-1726/18/4/045013>
19. Y. Ando, X. Zhao, H. Shimoyama, G. Sakai, and K. Kaneto, *Int. J. Inorg. Mater. Sci.* **1**, 77 (1999). [https://doi.org/10.1016/S1463-0176\(99\)00012-5](https://doi.org/10.1016/S1463-0176(99)00012-5)
20. R. Andrews and M. C. Weisenberger, *Curr. Opin. Solid State Mater. Sci.* **8**, 31 (2004).
<https://doi.org/10.1016/j.cossms.2003.10.006>
21. N. P. Armitage, J. C. P. Gabriel, and G. Gruner, *J. Appl. Phys.* **95**, 3228 (2004).
<https://doi.org/10.1063/1.1646450>
22. S. S. Kulkarni, P. B. Belavi, and U. V. Khadke, *AIP Conf. Proc.* **1953**, ID 090046 (2018).
<https://doi.org/10.1063/1.5032893>
23. E. P. Giannelis, *Adv. Mater.* **8**, 1 (1996). <https://doi.org/10.1002/adma.19960080104>
24. A. Sharma, S. S. Kulkarni, and U. V. Khadke, *AIP Conf. Proc.* **2269**, ID 030090 (2020).
<https://doi.org/10.1063/5.0019654>
25. M. Biswas and S. S. Ray, *Adv. Polym. Sci.* **155**, 167 (2001). https://doi.org/10.1007/3-540-44473-4_3
26. X. Wei, G. Zhu, J. Fang, and J. Chen, *Int. J. Photoenergy* **2013**, ID 726872 (2013).
<https://doi.org/10.1155/2013/726872>
27. S. Devikala, P. Kamaraj, and M. Arthanareeswari, *Int. J. Sci. Res.* **3** (2013).
28. P. I. Devi and K. Ramachandran, *J. Experiment. Nano Sci.* **6**, 281 (2011).
<https://doi.org/10.1080/17458080.2010.497947>
29. A. B. D. Nandiyanto, R. Oktiani, and R. Ragadhita, *Indonesian J. Sci. Technol.* **4** (2019).
<https://doi.org/10.17509/ijost.v4i1.15806>
30. W. Li, H. Li, and Y. –M. Zhang, *J. Mater. Sci.* **44**, 2977 (2009).
<https://doi.org/10.1007/s10853-009-3395-x>
31. W. C. Ganand and W. H. A. Majid, *Smart Mater. Struct.* **23**, ID 045026 (2014).
<https://doi.org/10.1088/0964-1726/23/4/045026>